

On the Alfvén wave cut-off in partly ionized collisional plasmas

J. Vranjes¹ and M. Kono²

¹Institute of Physics Belgrade, Pregrevica 118, 11080 Zemun, Serbia,

Email: jvranjes@yahoo.com

²Faculty of Policy Studies, Chuo University, Tokyo, Japan,

Email: kono@fps.chuo-u.ac.jp

Abstract: The cut-off of the Alfvén wave, caused by plasma collisions with neutrals in multi-component partially ionized plasmas, is discussed. Full multi-component theory is used, and similarities and differences regarding the classic magnetohydrodynamic theory are presented. It is shown that the cut-off in partially ionized plasma in principle may remain the same as predicted in classic magnetohydrodynamic works, although multi-component theory also yields some essential differences. Due to electric field, the ion motion is intrinsically two-dimensional and this results in additional forced oscillations of neutrals. One new small parameter, containing the ion inertial length, appears in the multi-component theory. This new small parameter is missing in the magnetohydrodynamic description, and it turns out that for some parameters it may be greater than the ions-to-neutrals density ratio which is the only small parameter in the magnetohydrodynamic description. Due to this the Alfvén wave behavior can become much different as compared to classic magnetohydrodynamic results. It is shown also that in plasmas with unmagnetized ions, Alfvén waves cannot be excited. This by all means applies to the solar photosphere where the ion collision frequency may be far above the ion gyro-frequency.

1 Introduction

The magnetohydrodynamic (MHD) description of the cut-off in partially ionized plasma may be found in the work [1] and in many subsequent works [2, 3, 4]. In such a MHD description, the electron and ion components are treated as one single fluid and neutrals as the second one. Friction between the single-fluid plasma on one side, and neutrals on the other, causes damping of the Alfvén wave and this damping increases with the increased number of neutrals. The wave eventually becomes completely non-propagating when the amount of neutrals reaches certain critical value. Alternatively, the same effect appears for increasing the wave-length or wave-period because a plasma particle suffers more and more collisions within one wave oscillation. However, by increasing the number of neutrals (or for a greater wave-length or wave-period) the mode is shown to re-appear again and it may propagate with a very weak damping. In such a regime the plasma and

neutrals are collisionally so strongly coupled that there is no friction between them any longer and they move together as a true single fluid.

However, it is frequently overlooked that in this strongly coupled regime, in which neutrals participate in the wave motion, the total fluid density is much greater. Some initial small electromagnetic perturbations involve the motion of charged species first, and only after some mean collisional time the neutrals are set into motion as well. This all may happen only on the account of the initial energy of the perturbation. Therefore, the initial wave amplitude becomes drastically reduced. In other words, the phase speed of the initial perturbation (for time interval shorter than the collisional time) is necessarily the Alfvén speed containing the plasma density only. After the collisional time, the Alfvén speed includes total (plasma plus neutrals) density, and the wave amplitude and flux become drastically reduced. These features have been overlooked recently in [5] resulting in the wave flux which is several orders of magnitude larger from what may be expected in reality [6].

In a recent study [7] the authors claimed that i) the cut-off obtained in classic MHD works which they cite was un-physical, ii) it was not an intrinsic property of the wave, and iii) it could naturally be removed when the Hall and inertia terms are taken into account. We shall show that the classic MHD cut-off cannot be removed by these terms. We shall use full three component equations which naturally incorporate all ‘additional terms’ which they propose as extra physics within their hybrid MHD-fluid model. Several completely new features of the Alfvén wave appear in a fully multi-component analysis which we present, and these can not be predicted within the MHD theory. In addition, we shall show that Alfvén waves cannot be excited in the lower solar atmosphere due to the fact that ions are un-magnetized. This has profound implications on the coronal heating model based on the Alfvén waves that are assumed massively produced by convective motions in the lower solar atmosphere.

2 The Alfvén wave in partially ionized plasmas

The physics of partially ionized plasma is considerably richer as compared to the fully ionized one. Some different type of collisions appear, the system becomes intrinsically multi-component, particles may be lost and re-created, etc. Therefore before discussing the collisional damping of the Alfvén wave in such an environment it is necessary to provide accurate collisional cross sections for collisions of interest here. We shall take ions to be protons, and neutrals are parental hydrogen atoms.

In Fig. 1 we give the cross sections for proton collisions with neutral hydrogen obtained from quantum theory, in the range 0.05 – 1.5 eV proton energy in the center of mass (CM) frame (bottom x -axis). In the laboratory (plasma) frame the energy range 0.1 – 3 eV is

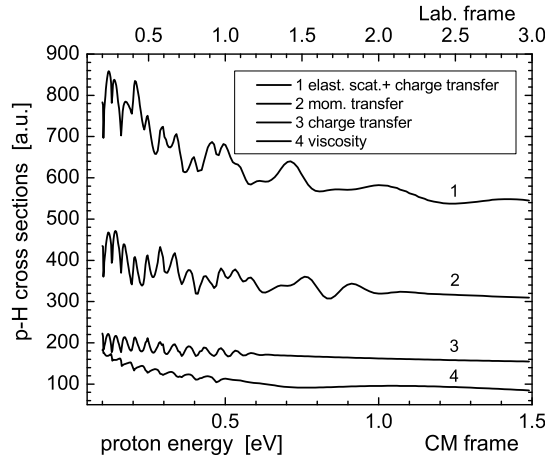


Figure 1: Integral cross sections σ_{pH} (in units a.u. = $2.8 \cdot 10^{-21} \text{ m}^2$) for proton collisions with neutral hydrogen H in terms of proton energy and for the model of quantum-mechanically indistinguishable particles, from [8, 9, 10, 11].

given by the top x -axis using the transformation formula $E_{lab} = E_{CM}(m_1 + m_2)/m_2$, where m_2 is the target particle. It provides the following important features: a) velocity (energy) dependent cross sections, b) different cross sections for different phenomena (elastic scattering, momentum transfer, charge exchange, viscosity), c) the charge exchange as a specific sort of inelastic collisions that cannot be omitted in systems containing both ions and their parental atoms. These three features are rarely seen studied in space plasmas, separately or together. In the present context they have never been studied in the past. It will be shown below that this is the only proper approach.

In application to the solar atmosphere, the energy dependence [the feature a)] in the present study is equivalent to the altitude (i.e., temperature) dependence in the stratified solar plasma. The four different lines [the feature b)] describe different cross sections: the sum of elastic scattering and charge exchange (line 1), momentum transfer (line 2), charge exchange alone (line 3), and viscosity (line 4). The values presented here are the most accurate that exist. The physics of this difference between various cross sections is described partly in a recent work [11] and in much more detail in [10, 12], and in [13]. The quantum-mechanical indistinguishability of particles used here implies overlapping of particle quantum wave functions at low energies. As described in [10], when the nuclei are identical and the collision energy is relatively low, in the process of collisions it is not possible to distinguish the ion which is elastically scattered from the ion which originates from charge transfer unless they are additionally labeled (e.g., by their spin). For this reason the line 1 in Fig. 1 contains the sum of the elastic scattering and the charge exchange cross sections. This total cross section should be used in the estimate of magnetization of plasma particles, while for example the cross section for momentum transfer is to be used in the friction force terms. More details on this issue may be found in [11].

The lines for the momentum transfer and viscosity cross sections are obtained after an integration over the scattering angle θ similar to the line 1, but weighted by $1 - \cos\theta$ and $\sin^2\theta$, respectively. This describes essentially different physics involved in the momentum transfer and viscosity, therefore the different lines in Fig. 1. In the case of viscosity this emphasizes the scattering at the angle $\pi/2$ and de-emphasizes the forward and backward ones, while the factor $1 - \cos\theta$ in the momentum transfer emphasizes the backward scattering angles. Note also that elastic scattering is typically forward, and charge exchange backward scattering process. We stress that both the momentum transfer and the viscosity lines also contain the contribution from the charge exchange effect. In practical application further in the text, this also implies that in the given approach in describing plasma wave dynamics we shall have one single ‘friction force’ term which determines the total wave damping on neutrals, instead of two separate terms as typically seen in the literature, one for friction force caused by elastic collisions and one for the momentum lost (or gained) due to charge exchange. This all not only yields much more accurate results (in view of the most reliable cross sections we use) but also considerably simplifies derivations as will become clear below.

We note that, following the recipe from [8], the commonly used (classic) elastic scattering differential cross sections may be obtained as the absolute value of the difference of the total (elastic plus charge transfer) differential cross section which is in the basis of the model we use here, and charge transfer differential cross section. With this we can then calculate the integral quantities (i.e., momentum transfer and viscosity cross sections) in order to obtain results for the right classical limit. As described in [8], this limit implies the model of distinguishable particles.

It should be stressed again that partially ionized plasmas like the lower solar atmosphere contain ions and corresponding parental neutral atoms, so the charge exchange cannot possibly be omitted [the feature c)]. In laboratory conditions in inert gases (helium, neon, argon) the charge exchange cross section is the largest one [14]. In the case of hydrogen it is below the cross section for elastic scattering. However, because of the described specific angle dependence of the charge transfer from one side, and rather different angle dependence of the other three cross sections in Fig. 1 from the other side, it contributes considerably (and differently) to all three of them. Therefore the procedure presented here has no alternative, it has been tested in numerous works in the past like in the references mentioned above, and it gives values in complete agreement with laboratory measurements, e.g., in [15].

In what follows we shall also need the momentum transfer cross section for electron-hydrogen collisions. Some values of the cross section in the energy (temperature) range of interest here are given in Table 1, from [16].

To proceed with the Alfvén wave cut-off, we use fully three component theory without

Table 1: Cross section for momentum transfer for e-H collisions, following [16].

el. energy [eV]	0.2	0.3	0.5	0.7	1
$\sigma_{eH,mt} [\times 10^{-19} \text{ m}^2]$	3.7	3.1	3	2.8	2.5

any assumptions following the procedure that may be found in standard textbooks (e.g. [17]) for the shear Alfvén wave. We take $\vec{B}_0 = B_0 \vec{e}_z$, and in such a geometry both ion and electron fluids oscillate together in the direction of the perturbed magnetic field vector $\vec{B}_1 = B_1 \vec{e}_y$. This is due to the $\vec{E}_1 \times \vec{B}_0$ drift, which separates neither charges nor masses. The direction of the electric field is determined by the Faraday law. The wave is further sustained by the additional polarization drift $\vec{v}_{pj} = (m_j/q_j B_0^2) \partial \vec{E}_1 / \partial t$ and the consequent Lorentz force $j_x \vec{e}_x \times \vec{B}_0$, which is again in the y -direction and has a proper phase shift. The polarization drift appears as a higher order term due to $|\partial/\partial t| \ll \Omega_i$. It introduces the ion inertia effects and if it is neglected, then the Alfvén wave vanishes. The wave thus develops at time scales far greater than the ion gyro-rotation time, and equivalently at spatial scales far exceeding the ion gyro-radius. The mode is fully described by the wave equation which is obtained by combining Ampère and Faraday law equations

$$\nabla \times (\nabla \times \vec{E}) + \mu_0 \frac{\partial \vec{j}}{\partial t} = 0, \quad (1)$$

where the displacement current is omitted as appropriate for phase speed far below the speed of light. The plasma current is calculated by using the linearized momentum equations for ions and electrons

$$m_i n_0 \frac{\partial \vec{v}_i}{\partial t} = e n_0 (\vec{E} + \vec{v}_i \times \vec{B}_0) - m_i n_0 \nu_{ie} (\vec{v}_i - \vec{v}_e) - m_i n_0 \nu_{in} (\vec{v}_i - \vec{v}_n), \quad (2)$$

$$m_e n_0 \frac{\partial \vec{v}_e}{\partial t} = -e n_0 (\vec{E} + \vec{v}_e \times \vec{B}_0) - m_e n_0 \nu_{en} (\vec{v}_e - \vec{v}_n) - m_e n_0 \nu_{ei} (\vec{v}_e - \vec{v}_i), \quad (3)$$

and the corresponding equation for neutrals

$$\frac{\partial \vec{v}_n}{\partial t} = -\nu_{ne} (\vec{v}_n - \vec{v}_e) - \nu_{ni} (\vec{v}_n - \vec{v}_i). \quad (4)$$

Here, the static quasi-neutral equilibrium without macroscopic flows is assumed and the equilibrium quantities are denoted by the subscript 0. The last terms in Eqs. (2, 4) describe the momentum change due to $p-H$ collisions and it includes the contribution from both elastic collisions and charge exchange, i.e., the corresponding collision frequency includes the momentum transfer collision cross section σ_{mt} (line 2 from Fig. 1), $\nu_{in} = \sigma_{mt} n_{n0} v_{Ti}$. The momentum conservation in Eq. (4) implies

$$\nu_{ni} = m_i n_{i0} \nu_{in} / (m_n n_{n0}), \quad \nu_{ne} = m_e n_{e0} \nu_{en} / (m_n n_{n0}). \quad (5)$$

Further in the text we shall use $m_n = m_i$. In charge exchange collisions the number of protons and neutrals does not change so there is no source-sink term in the continuity equation and the latter in the cold plasma case becomes redundant. However, a source-sink momentum change appears in the momentum equation through σ_{mt} which contains contribution from the charge transfer. In such collisions a proton takes over one electron from the hydrogen atom. The latter then becomes charged and is consequently directly involved in the wave motion, yet it does not share the same momentum as the other protons and some wave energy must be spent in order to set it into motion. Similarly, the described proton which becomes neutral atom takes away a part of the momentum previously gained from the wave. All these effects are now self-consistently introduced. It should be stressed that very frequently in the literature the friction force term appears separately from the term which describes the momentum change by the charge exchange, see for example in works [18] and [19]. The two forces are given by $\vec{F}_f = m_i n_i \nu_1 v_{Ti} (\vec{v}_i - \vec{v}_n)$ and $\vec{F}_{cx} = m_i n_n \nu_2 v_{Ti} (\vec{v}_i - \vec{v}_n)$ where $\nu_1 = \sigma_1 n_n v_{Ti}$, $\nu_2 = \sigma_2 n_i v_{Ti}$, and $\sigma_{1,2}$ should be calculated following the model of distinguishable particles as described previously in this section. The total force reduces to $\vec{F} = m_i n_i (\sigma_1 + \sigma_2) v_{Ti} (\vec{v}_i - \vec{v}_n)$ where now the sum of the cross sections corresponds to our σ_{mt} . In such an approach equations are more complicated and a great care is needed so that the corresponding collision frequencies are calculated correctly.

Due to the absence of the source-sink terms in the continuity equations, and also in order to keep the present model close to those from [1] and [7], the density perturbations, thermal effects and viscosity are neglected. So the number densities in Eqs. (2-4) describe the equilibrium quantities and we shall take care that we are in the correct wave phase speed range to satisfy such an assumption (roughly speaking in the small plasma- β limit). Hence, Eqs. (1-4) together with the quasi-neutrality condition which is used $n_i = n_e = n_0$ make a closed set.

We stress that a complete comparison of our model and results with those available in the literature (including the above cited two references) is not possible due to the following reasons. Even if we would disregard the charge exchange, there remains the fact that typical models, presently (and previously) widely used in the literature, make no distinction between the cross sections for momentum transfer and elastic scattering. However, these two cross sections are different, and the charge exchange additionally (and differently) contributes to both of them. These facts make the theory we provide here much more accurate in comparison to what may be found in the literature.

2.1 Classic MHD derivation

In order to obtain the classic result of [1] and for comparison with our results later in text, the electron and ion momentum equations are summed, their mutual friction vanishes, there appears the current in the Lorentz force term which is then expressed through the magnetic field from the Ampère law. The resulting momentum equation is

$$\begin{aligned} m_i n_i \frac{\partial \vec{v}_i}{\partial t} + \underline{m_e n_e \frac{\partial \vec{v}_e}{\partial t}} = \underline{e(n_i - n_e) \vec{E}} + \frac{1}{\mu_0} (\nabla \times \vec{B}) \times \vec{B} \\ - m_i n_i \nu_{in} (\vec{v}_i - \vec{v}_n) - \underline{m_e n_e \nu_{en} (\vec{v}_e - \vec{v}_n)}. \end{aligned} \quad (6)$$

The underlined terms are further omitted, and what remains is combined with the neutral equation (4) where the electron contribution is omitted as well. The system is closed with the induction equation

$$\frac{\partial \vec{B}}{\partial t} = \nabla \times (\vec{v} \times \vec{B}), \quad (7)$$

where for \vec{v} the ion speed is used. This yields the well known cubic dispersion equation [1]:

$$\omega^3 - \omega k^2 c_a^2 + i \nu_{in} \left[\left(1 + \frac{n_0}{n_{n0}} \right) \omega^2 - k^2 c_a^2 \frac{n_0}{n_{n0}} \right] = 0. \quad (8)$$

Dispersion equation (8) contains one small parameter n_0/n_{n0} (here and further in the text the medium is assumed as weakly ionized). It is solved numerically for the following arbitrary parameters: $B_0 = 0.05$ T, $n_0 = 1.1 \cdot 10^{17}$ m⁻³, $n_{n0} = 6.8 \cdot 10^{19}$ m⁻³, $T = 5755$ K. This yields $\Omega_i = 4.8 \cdot 10^6$ Hz, and with the help of Fig. 1 we have $\nu_{in} = 4.88 \cdot 10^5$ Hz for the momentum transfer. Note that these parameters in fact describe plasma in the chromosphere at altitude 900 km, although the assumed magnetic field may be too strong. However, this is immaterial for the present purpose as we only want to describe basic features of the classic MHD result, and to compare it with the multi-component description later in the text. The Kulsrud-Pearce (KP) complex frequency is calculated from Eq. (8) and presented in Fig. 2. The real part of the frequency vanishes above the critical wave length $\lambda_{c1} \simeq 84.35$ m, and re-appears again for wave lengths above $\lambda_{c2} \simeq 521.5$ m. The damping in the short wave length region A is almost constant $\gamma \simeq \nu_{in}/2 \simeq 2.44 \cdot 10^5$ Hz as can be deduced also analytically from Eq. (8). In the upper propagation window C in most of the spectrum we have roughly $\gamma \sim 1/\nu_{in}$, and this too can be analytically deduced from Eq. (8).

Several comments are in order. With the assumed geometry $\vec{B}_1 \equiv B_y \vec{e}_y$, it is seen that after neglecting the underlined terms in Eq. (6), the motion of the ion center of mass is strictly one-dimensional because $(\nabla \times \vec{B}_1) \times \vec{B}_0$ is parallel to \vec{v}_{i1} . This is completely different as compared with our multi-component model later in the text where the motion of the ion center mass is essentially two-dimensional. The reason for difference is clearly the fact that the electric field vanishes from Eq. (6). ‘Vanishing’ of electric field only tells

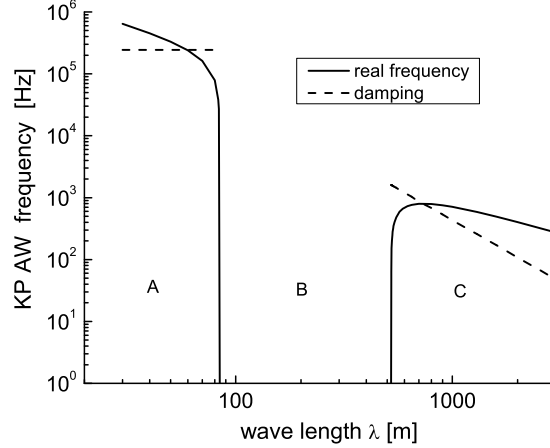


Figure 2: Kulsrud-Pearce solution $\omega = \omega_r - i\gamma$ of Eq. (8) for parameters given in the text.

us that *electric force* (as a vector), when acting on total plasma (e+i) is zero. Physically this means simply that opposite charges suffer equal force with opposite direction and nothing else, while in fact the electric force acting on ions and electrons separately is still present. Observe that in Eq. (6) the contribution of the electric force vanishes only because of quasi-neutrality and not because of actual absence of the electric field. In other words, the electric field is always present and the motion of electrons and ions is fully two-dimensional in perpendicular direction, yet this information is lost in the KP-MHD equation. The presence of the electric field is logical because it is there due to electromagnetic perturbation, and this even without plasma. In other words, magnetic field is disturbed in y -direction and the Faraday law then tells us that there is electric field in x -direction (even without plasma).

Observe also that the KP model is based on an ideal frozen-in environment for the magnetic field [this is incorporated in the induction equation (7)]. This also implies that the only current which was initially in the Lorentz force $\sim \vec{j} \times \vec{B}$, was in fact the ion polarization drift current $\vec{v}_{p,i} \sim \vec{E}_x \vec{e}_x$ [this is because the other, more dominant, $\vec{E} \times \vec{B}$ -drift is the same for electrons and ions, so the plasma motion in y -direction is current-less]. Hence, although the starting momentum equation *implies* two-dimensional motion (that is the polarization drift in x -direction and $\vec{E} \times \vec{B}$ -drift in y -direction), from Eq. (6), without underlined terms, we have a purely one-dimensional ion dynamics. This is just one out of many contradictions that are inherent to the MHD model, some others may be seen in the work [20].

2.2 Approximate analytical approach

Using an approximate method we shall now demonstrate that there can be no Alfvén wave if ions are un-magnetized. Although self-evident, this fact is frequently ignored and

Alfvén waves have been studied in lower solar atmosphere where ion collision frequency (above 10^9 Hz) far exceeds the ion gyro-frequency, and where these waves cannot possibly be excited.

Because of lengthy expressions, in this section we may take ion collisions with neutrals most dominant, which is easily satisfied in the lower solar atmosphere [11]. From the ion equation (2) we may first express the perpendicular ion speed from the friction force term:

$$\vec{v}_{\perp i} = \frac{e\vec{E}_1}{m_i\nu_{in}} + \frac{e}{m_i\nu_{in}}\vec{v}_{\perp i} \times \vec{B}_0 - \frac{1}{\nu_{in}}\frac{\partial\vec{v}_{\perp i}}{\partial t} + \vec{v}_{\perp n}. \quad (9)$$

Next, we make vector product $\vec{e}_z \times$ of Eq. (2) and express the ion perpendicular speed from the Lorentz force term:

$$\begin{aligned} \vec{v}_{\perp i} = & -\frac{1}{B_0}\vec{e}_z \times \vec{E}_1 + \frac{\nu_{in}}{\Omega_i}\vec{e}_z \times \vec{v}_{\perp i} + \frac{1}{\Omega_i}\frac{\partial}{\partial t}\vec{e}_z \times \vec{v}_{\perp i} \\ & - \frac{\nu_{in}}{\Omega_i}\vec{e}_z \times \vec{v}_{\perp n}. \end{aligned} \quad (10)$$

The neutral speed is eliminated by using Eq. (4) which yields

$$\vec{v}_{\perp n} = \frac{i\nu_{ni}}{\omega + i\nu_{ni}}\vec{v}_{\perp i}. \quad (11)$$

Here, the momentum transfer due to neutral-electron collisions is omitted as higher order in comparison to their collision with ions. The two expressions for the ion speed are made equal, and the vector product $\vec{e}_z \times$ is again applied on the resulting equation. This yields the following recurrent formula with the small parameter $|\partial/\partial t|/\Omega_i \ll 1$:

$$\begin{aligned} \vec{v}_{\perp i} = \alpha_i \left(& -\frac{1}{B_0}\vec{e}_z \times \vec{E}_1 + \frac{\nu_{in}}{\Omega_i}\frac{\vec{E}_1}{B_0} + \frac{1}{\Omega_i}\vec{e}_z \times \frac{\partial\vec{v}_{\perp i}}{\partial t} \right. \\ & \left. - \frac{\nu_{in}}{\Omega_i^2}\frac{\partial\vec{v}_{\perp i}}{\partial t} + \frac{i\nu_{in}^2\nu_{ni}}{\Omega_i^2\omega_n}\vec{v}_{\perp i} - \frac{i\nu_{in}\nu_{ni}}{\Omega_i\omega_n}\vec{e}_z \times \vec{v}_{\perp i} \right). \end{aligned} \quad (12)$$

Here, $\omega_n = \omega + i\nu_{ni}$, and $\alpha_i = 1/(1 + \nu_{in}^2/\Omega_i^2) \leq 1$. Eq. (12) will further be discussed for two separate cases.

2.2.1 Small ratio $\nu_{ni}/|\omega_n|$. Explicit absence of Alfvén wave for un-magnetized ions

In the case when ν_{in}/Ω_i is arbitrary but finite, the first two terms on the right-hand side in Eq. (12) may be assumed as leading order, and applying standard approximate procedure they can be used to replace $\vec{v}_{\perp i}$ in the remaining four terms. In the same time the following small ratio is assumed in the last two terms in Eq. (12):

$$\nu_{ni}/|\omega_n| \ll 1. \quad (13)$$

This condition can easily be satisfied in view of Eq. (5) and for a weakly ionized environment where $n_0/n_{n0} \ll 1$, although it is not so general. With this the recurrent formula (12) remains valid and after a few steps this yields

$$\begin{aligned} \vec{v}_{\perp i} = \alpha_i \left\{ -\frac{\vec{e}_z \times \vec{E}_1}{B_0} \left(1 + \frac{i2\alpha_i \nu_{in} \omega}{\Omega_i^2} + \frac{i2\alpha_i \nu_{in}^2 \nu_{ni}}{\Omega_i^2 \omega_n} \right) \right. \\ \left. + \frac{\vec{E}_1}{B_0} \left[\frac{\nu_{in}}{\Omega_i} - \frac{i\alpha_i \omega}{\Omega_i} \left(1 - \frac{\nu_{in}^2}{\Omega_i^2} \right) - \frac{i\alpha_i \nu_{in} \nu_{ni}}{\Omega_i \omega_n} \left(1 - \frac{\nu_{in}^2}{\Omega_i^2} \right) \right] \right\}. \end{aligned} \quad (14)$$

For the present purpose it may be good enough to omit electrons and their collisions completely. For large time and space scales of interest here, the mobile electrons will closely follow the ion dynamics. On the other hand, their contribution to dragging (by friction) of the heavy background of neutrals is small in any case, as already assumed in Eq. (11). This will be confirmed later in the text, see Fig. 3. With such an approach we shall remain as close to the classic MHD theory as possible.

To make this point more clear, derivations for electrons can be repeated in a similar manner with the distinction that the left hand side of Eq. (3) is omitted, which is fully justified in view of the mass difference. This yields

$$\begin{aligned} \vec{v}_{\perp e} = \alpha_e \left(-\frac{\vec{e}_z \times \vec{E}_1}{B_0} - \frac{\nu_e}{\Omega_e} \frac{\vec{E}_1}{B_0} + \frac{\nu_{en}}{\Omega_e} \vec{e}_z \times \vec{v}_n + \frac{\nu_e \nu_{en}}{\Omega_e^2} \vec{v}_n \right. \\ \left. + \frac{\nu_{ei}}{\Omega_e} \vec{e}_z \times \vec{v}_i + \frac{\nu_e \nu_{ei}}{\Omega_e^2} \vec{v}_i \right). \end{aligned} \quad (15)$$

Here, $\alpha_e = 1/(1 + \nu_{en}^2/\Omega_e^2) \simeq 1$, $\nu_e = \nu_{ei} + \nu_{en}$. In Eq. (15) collisions with both ions and neutrals are formally kept, and in principle the neutral and ion speeds here should be calculated from full Eqs. (2,4) to satisfy conservation laws, but this will not be necessary as shown below.

For the wave equation (1) we need only x -component of Eqs. (14, 15). We may also take $\nu_{en} > \nu_{ei}$, this will not affect generality of conclusions below. So now we may compare the leading x -term from the electron equation (that is the second term) with any of the x -terms from the ion equation (and we take the second term again). These two yield the following contribution to the current in the wave equation

$$\left(\alpha_i \frac{\nu_{in}}{\Omega_i} + \alpha_e \frac{\nu_{en}}{\Omega_e} \right) \frac{E_x}{B_0} = n_{n0} (\alpha_i \sigma_{in} \rho_i + \alpha_e \sigma_{en} \rho_e) \frac{E_x}{B_0}.$$

From Table 1 and from Fig. 1 (see the line 2 there), for energies of interest here we have always $\sigma_{in} > \sigma_{en}$, while in the same time $\rho_i \gg \rho_e$. Hence, as long as $\alpha_i > \alpha_e (\rho_e/\rho_i) (\sigma_{en}/\sigma_{in})$ the electron contribution can completely be neglected. This condition is easily satisfied if we allow the ratio ν_{in}^2/Ω_i^2 to be finite (with any of the two possibilities: $\nu_{in}^2/\Omega_i^2 > 1, < 1$), so that $\alpha_i \leq 1$, while $(\rho_e/\rho_i) (\sigma_{en}/\sigma_{in}) \ll 1$ and $\alpha_e \leq 1$ or $\alpha_e \simeq 1$.

Observe that keeping electron inertia term would yield electron polarization current in the x -direction, but it is proportional to the electron mass and indeed negligible as we assumed above [see also Eq. (33) in the following section].

Consequently, we may indeed proceed by omitting electrons and for the ion x -component we have

$$v_{ix} = \frac{\alpha_i \vec{E}_1}{B_0} \left[\frac{\nu_{in}}{\Omega_i} - \frac{i\alpha_i}{\Omega_i} \left(1 - \frac{\nu_{in}^2}{\Omega_i^2} \right) \left(\omega + \frac{\nu_{in}\nu_{ni}}{\omega_n} \right) \right]. \quad (16)$$

From Eqs. (1, 16) the following approximate dispersion equation is obtained:

$$\begin{aligned} \omega^2 (\nu_{in}^2 - \Omega_i^2) - i\omega\nu_{in} (\nu_{in}^2 + \Omega_i^2) + k^2 \lambda_i^2 (\nu_{in}^2 + \Omega_i^2)^2 \\ + \nu_{in}\nu_{ni} (\nu_{in}^2 - \Omega_i^2) = 0. \end{aligned} \quad (17)$$

In the absence of collisions this yields a real Alfvén mode $\omega^2 = k^2 c_a^2$. On the other hand, in particular case when $\nu_{in} = \Omega_i$ we obtain

$$\omega = -i2k^2 \lambda_i^2 \nu_{in}, \quad \lambda_i = c/\omega_{pi}.$$

Hence, no real mode exists in this case.

In the presence of collisions in general, Eq. (17) has no real solutions if ions are *unmagnetized*:

$$\nu_{in} \geq \Omega_i. \quad (18)$$

On the other hand, for weakly magnetized ions $\nu_{in} < \Omega_i$ from Eq. (17) we obtain very approximately that real solutions are possible provided that

$$\frac{\Omega_i}{\nu_{in}} > \frac{1}{2k\lambda_i}. \quad (19)$$

The condition (19) determines the Alfvén wave cut-off for waves satisfying the condition (13).

The condition (13) clearly includes the case $\nu_{ni} = 0$ as well. From our starting equation (4) with omitted electron effects we see that this is equivalent to assuming neutrals as a static background (fairly well justified for short wavelengths). In this case Eq. (17) reveals that there can be no Alfvén wave for unmagnetized ions $\nu_{ni} > \Omega_i$.

2.2.2 Arbitrary ratio $\nu_{ni}/|\omega_n|$

We shall now repeat the approximate procedure with the only condition

$$\frac{|\omega|}{\Omega_i} \ll 1. \quad (20)$$

In Eq. (14) we eliminate the terms with the vector product $\vec{e}_z \times \vec{v}_{\perp i}$ by using Eq. (10). After a few steps this yields

$$\vec{v}_{\perp i} = -\frac{\delta_i}{B_0} \vec{e}_z \times \vec{E}_1 + \delta_i \frac{\omega}{\Omega_i} \left(\frac{\nu_{in}}{\omega_n} - i \right) \frac{\vec{E}_1}{B_0}$$

$$\begin{aligned}
& + 2\delta_i \frac{\omega}{\Omega_i} \frac{\nu_{in}}{\Omega_i} \left(\frac{\nu_{ni}}{\omega_n} + i \right) \vec{v}_{\perp i}, \quad \delta_i = \frac{\alpha_i}{\beta_i \gamma_i}, \\
\beta_i &= 1 - i\alpha_i \frac{\nu_{ni}}{\omega_n} \frac{\nu_{in}^2}{\Omega_i^2}, \quad \gamma_i = 1 - \frac{\alpha_i}{\beta_i} \frac{\nu_{ni}}{\omega_n} \frac{\nu_{in}^2}{\Omega_i^2} \left(i + \frac{\nu_{ni}}{\omega_n} \right).
\end{aligned} \tag{21}$$

Because of the small ratio (20), the first term on the right-hand side in the recurrent formula (21) is the leading order one, so it is used in the last term. From the resulting equation we need only v_x in the wave equation

$$k^2 E_x - ien_0\mu_0\omega v_x = 0.$$

Hence,

$$v_x = \delta_i \frac{\omega}{\Omega_i} \left(\frac{\nu_{in}}{\omega_n} - i \right) \frac{E_1}{B_0}$$

is used in the wave equation yielding the following approximate dispersion equation

$$\begin{aligned}
& \omega^4 + i\omega^3(\nu_{in} + 2\nu_{ni}) - \omega^2(\nu_{in}\nu_{ni} + \nu_{ni}^2 + k^2\lambda_i^2\nu_{in}^2 + k^2c_a^2) \\
& - 2i\nu_{ni}k^2c_a^2\omega + k^2c_a^2\nu_{ni}^2 = 0.
\end{aligned} \tag{22}$$

Contrary to [1] result (8), the obtained equation is 4th order. It describes a) the Alfvén wave, and b) some low frequency forced neutrals' (FN) oscillations due to their coupling with plasma. These FN oscillations appear only due to the fact that the induced neutral motion is two-dimensional. Setting $v_{ny} = 0$ or $v_{nx} = 0$ yields a third order equation instead of Eq. (22), which is then equivalent to the result of [1] and [2], so the FN collisional mode vanishes. In similar studies with friction related to the ion acoustic (IA) waves [21] this extra collisional mode does not appear; the neutral response for longitudinal IA waves is one-dimensional. We stress that FN mode describes forced oscillations and not a normal mode in a neutral gas, it is caused by coupling of neutrals with plasma but propagates independently of plasma modes and this only in the neutral gas (see also [22]). To get a rough glimpse of the FN mode we may write Eq. (22) as $D(\omega_r + i\gamma, k) \equiv D_r + iD_{im} = 0$. Knowing that the spectrum (number of modes) must be determined by the real part, we may set $D_r = 0$ which then yields an obvious Alfvén wave part and additional terms describing the FN mode, and some coupling terms. Assuming that the AW part is weakly affected by the FN mode and that frequencies of the two modes are well separated, in the equation $D_r = 0$ we may set the Alfvén part separately equal to zero. The remaining terms yield very roughly

$$\omega^2 \simeq \frac{\epsilon^2 k^2 c_a^2}{\epsilon + k^2 \lambda_i^2}, \quad \epsilon = \frac{n_0}{n_{n0}}. \tag{23}$$

This expression describes the FN mode accurately only in the long wavelength limit and where the AW is absent, see Sec. 3.1. In the short wavelength regime it gives the frequency which is far from actual values because the mode is very strongly damped and

many essential terms from the imaginary part of (22) are missing in the given expression. But note the presence of two small terms in Eq. (23), the previously obtained (within the MHD approach) ϵ , and the new one $k^2\lambda_i^2$. Further in the text it will be shown that the interplay of these two is crucial for the Alfvén wave behavior.

Observe that the BGK integral used in derivations is the same for both Kulsrud-Pearce and our multi-component model, therefore it should give similar results in the two descriptions. However, it will be shown in Sec. 3.1 that this is dependent on parameters and in some cases the results are essentially different.

Eq. (22) will be discussed together with Eqs. (24, 29) which are presented later in the text. It will be shown that, depending on parameters, the two propagation windows A and C from Fig. 2 and the AW cut-off may remain intact as predicted in [1], contrary to recent claims [7].

2.3 Ion-neutral plasma without approximations

In the wave equation we need x -component of the perturbed speed so neglecting contribution of electrons in starting equations Eqs. (1-4) and keeping all remaining terms, thus without approximations based on the recurrent formula (12), yields the following dispersion equation:

$$\begin{aligned} & \omega^4 \left(1 + k^2\lambda_i^2\right) + i\omega^3 \left[\nu_{in} + 2\nu_{ni} + 2k^2\lambda_i^2 (\nu_{in} + \nu_{ni})\right] \\ & - \omega^2 \left[\nu_{in}\nu_{ni} + \nu_{ni}^2 + k^2c_a^2 + k^2\lambda_i^2(\nu_{in} + \nu_{ni})^2\right] - i2k^2c_a^2\nu_{ni}\omega \\ & + k^2c_a^2\nu_{ni}^2 = 0. \end{aligned} \tag{24}$$

Clearly this is very similar to Eq. (22) obtained above from the recurrent formula, with a few additional but unessential terms, and it describes again the Alfvén wave modified by collisions, and the FN mode. In view of omitted electrons, this is also equivalent to the KP equation (8), but compare the order of these two equations.

We stress again that although both electrons and ions contribute to these neutral oscillations, the electron contribution is completely negligible as will be shown quantitatively in the following section. Eq. (24) is solved numerically in the following section.

2.4 Full multi-component model with complete electron contributions

We now perform derivations for full three-component case with electron dynamics and all collisions included. Note that following the usual procedure, Eqs. (1-4) can be transformed and combined yielding the standard MHD equations used in [1], and in [7], including the generalized Ohm's law with additional terms which, according to [7] remove the

cut-off. Hence, all these ‘additional’ terms are naturally already present in our fully multi-component set of equations (1-4). Discussion about these additional terms in fact serves the purpose only within the MHD modeling which works well within known limits, but as an approximate theory it omits some physics, and such additions are used to re-introduce back the physics which is removed initially by reducing natural multi-component equations to the single-fluid MHD model. The issue of the Hall term is discussed in detail in Appendix A.

Using momentum conservation $m_n n_{n0} \nu_{nj} = m_j n_0 \nu_{jn}$ and $m_i = m_n$, from Eq. (4) we have the velocity of neutrals

$$\vec{v}_n = \frac{1}{\alpha} \frac{n_0}{n_{n0}} \left(\nu_{in} \vec{v}_i + \frac{m_e \nu_{en}}{m_n} \vec{v}_e \right), \quad (25)$$

$$\alpha = \nu_{en} \frac{m_e n_0}{m_n n_{n0}} + \nu_{in} \frac{n_0}{n_{n0}} - i\omega.$$

This is used in remaining derivations to eliminate the neutral speed. The electron and ion momentum equations become

$$\left[-i\omega m_e + m_e(\nu_{ei} + \nu_{en}) - \frac{n_0 m_e^2 \nu_{en}^2}{n_{n0} \alpha m_i} \right] \vec{v}_e = -e \vec{E} - e \vec{v}_e \times \vec{B}_0$$

$$+ \left(\nu_{ei} + \frac{\nu_{en} \nu_{in} n_0}{\alpha n_{n0}} \right) m_e \vec{v}_i, \quad (26)$$

$$\left(-i\omega + \nu_{in} + \frac{m_e \nu_{ei}}{m_i} - \frac{n_0 \nu_{in}^2}{n_{n0} \alpha} \right) \vec{v}_i = \frac{e}{m_i} \vec{E} + \frac{e}{m_i} \vec{v}_i \times \vec{B}_0$$

$$+ \left(\nu_{ei} + \frac{\nu_{en} \nu_{in} n_0}{\alpha n_{n0}} \right) \frac{m_e}{m_i} \vec{v}_e. \quad (27)$$

Hence, we now have a closed set of equations (1, 26, 27) for $\vec{v}_e, \vec{v}_i, \vec{E}$. This implies 5 scalar equations for $v_{ex}, v_{ey}, v_{ix}, v_{iy}, E_x$ which can be written as:

$$\begin{pmatrix} a_1 & eB_0 & -a_2 & 0 & e \\ -eB_0 & a_1 & 0 & -a_2 & 0 \\ -b_2 & 0 & b_1 & -\Omega_i & -\frac{e}{m_i} \\ 0 & -b_2 & \Omega_i & b_1 & 0 \\ ien_0\mu_0\omega & 0 & -ien_0\mu_0\omega & 0 & k^2 \end{pmatrix} \begin{pmatrix} v_{ex} \\ v_{ey} \\ v_{ix} \\ v_{iy} \\ E_x \end{pmatrix} = 0, \quad (28)$$

$$a_1 = -i\omega m_e + m_e(\nu_{ei} + \nu_{en}) - \frac{n_0 \nu_{en}^2 m_e^2}{\alpha n_{n0} m_i},$$

$$b_1 = -i\omega + \nu_{in} + \nu_{ei} \frac{m_e}{m_i} - \frac{n_0 \nu_{in}^2}{\alpha n_{n0}},$$

$$a_2 = m_e \left(\nu_{ei} + \frac{n_0 \nu_{en} \nu_{in}}{\alpha n_{n0}} \right), \quad b_2 = \frac{m_e}{m_i} \left(\nu_{ei} + \frac{n_0 \nu_{in} \nu_{en}}{\alpha n_{n0}} \right).$$

The complex frequency can be calculated by solving the dispersion equation

$$\Delta(\omega, k) = 0, \quad (29)$$

where Δ is determinant of the 5×5 square matrix in (28) whose meaning is obvious, and $k \equiv k_z$. The dispersion equation (29) without approximations is enormously lengthy (see Appendix B where a simplified version of it is given) and it is of the shape $a_6\omega^6 + ia_5\omega^5 + a_4\omega^4 + ia_3\omega^3 + a_2\omega^2 + ia_1\omega + a_0 = 0$. It describes the previous two modes [AW and forced neutral (FN) collisional mode] together with a high frequency mode due to electron inertia, which is of no importance for the present study. We shall deal with Eq. (29) numerically.

If collisions are completely neglected the dispersion equation which follows from complete Eqs. (1-3) (after neglecting terms of the order m_e/m_i with respect to unity) reads:

$$\omega^4 \left(k^2 + \frac{1}{\lambda_e^2} \right) - \omega^2 \Omega_e^2 \left(k^2 + \frac{1}{\lambda_i^2} \right) + \Omega_e^2 \Omega_i^2 k^2 = 0. \quad (30)$$

In the regime $\omega^2 \ll \Omega_i^2 \ll \Omega_e^2$, $\Omega_e = eB_0/m_e$, the first term may be neglected and this yields the collision-less Alfvén wave spectrum which can be written in two equivalent forms

$$\omega^2 = k^2 c_a^2 \left(1 - \frac{\omega^2}{\Omega_i^2} \right) \simeq k^2 c_a^2, \quad \text{or} \quad \omega^2 = \frac{k^2 c_a^2}{1 + k^2 \lambda_i^2} \simeq k^2 c_a^2. \quad (31)$$

In the regime $\omega^2 \gg \Omega_i^2$, the last term in (30) may be omitted and the resulting approximate expression gives the high frequency mode

$$\omega^2 \simeq \Omega_e \Omega_i \frac{1 + k^2 \lambda_i^2}{1 + k^2 \lambda_e^2}. \quad (32)$$

Frequency of this mode may exceed the electron plasma frequency and in this limit it would be appropriate to include electron density perturbations (and displacement current too) and to deal with the Langmuir and electromagnetic light modes as well. As may be seen further in the text, derivations are extremely lengthy already and we shall keep in mind the required frequency range for this third mode which will be present in derivations, so that we avoid additional modes.

It may also be seen that neglecting collisions and remaining in the AW frequency range, the x -component of the current in Eq. (1), i.e., the polarization current, yields the speed difference

$$v_{ix} - v_{ex} = \frac{i\omega}{\Omega_i} \frac{E_x}{B_0} \left(1 + \frac{m_e}{m_i} \right). \quad (33)$$

So the electron inertia term from the left-hand side of Eq. (3) is indeed negligible (yet it will be kept in the remaining calculations).

2.4.1 Numerical solutions of Eqs. (22, 24, 29)

In what follows we shall first show that all three equations (22, 24, 29) have practically the same solutions which for certain parameters further coincide with the Kulsrud-Pearce

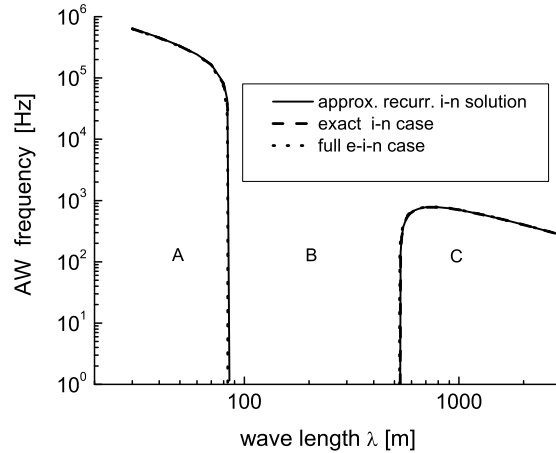


Figure 3: Real part of frequency $\omega = \omega_r - i\gamma$ for the strongly damped Alfvén wave as solution of Eqs. (22, 24, 29). The result is practically the same as Kulsrud-Pearce solution presented in Fig. 2.

result shown in Fig. 2. These three equations are solved for the same parameters used in Fig. 2, where now electron collisions are included through Eq. (29) with collision frequencies $\nu_{en} \simeq 6 \cdot 10^6$ Hz and $\nu_{ei} \simeq 9 \cdot 10^6$ Hz [c.f., Table 1 and also [11]]. The result for frequencies is given in Fig. 3. It shows that, contrary to claims in [7], the AW cut-off and classical results from [1] can also be obtained within the fully multi-component theory.

The differences between solutions of Eqs. (22, 24, 29) are very small and not visible in logarithmic scales used here, which also confirms that electron contribution to the damping and AW mode behavior is completely negligible as correctly assumed in the approximate equations (22, 24). The damping (which is not presented here) is very similar to the Kulsrud-Pearce solution given in Fig. 2.

The gap B, between the two propagation windows A and C in Fig. 3, can be controlled by several parameters. For example, taking $B_0 = 0.1$ T the short wavelength cut-off λ_{c1} is shifted towards $\lambda \simeq 168$ m, and the mode re-appears again at the long wavelength cut-off $\lambda_{c2} \simeq 1050$ m. However, in some cases, one of the propagation windows may vanish completely. However, this behavior cannot be obtained using the Kulsrud-Pearce equation (8), see more in Sec. 3.1.

In addition, the peculiar (and highly damped) forced neutral (FN) oscillations are presented in Fig. 4 for the same parameters as in Figs. 2, 3. Observe that it formally continues even for the wavelengths (up to 430 m) for which the frequency of its source (the Alfvén wave) has vanished (at around 80 m). To explain this, note that in the neutral equation (4) there is no explicit dependence on the wave length; such a dependence enters only through the ion speed which on the other hand is assumed spatially varying as $\exp(ikz)$. So dependence of FN mode on λ is only through its source, and the continuation of FN mode above the AW critical wave length λ_c is because it is the real part of the

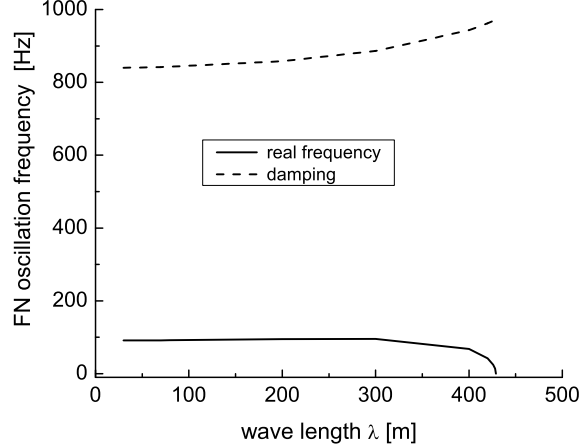


Figure 4: Frequency $\omega = \omega_r - i\gamma$ of forced neutral oscillations as additional solution of Eqs. (22, 24, 29) due to neutral friction with protons.

frequency of the AW which vanishes, not its imaginary part of its assumed wavelength. So what is left of the AW is spatial variation (defined by k) which decreases exponentially in time. The remaining imaginary part of the AW frequency enters the expression for polarization drift (10) and this provides the necessary two-dimensionality in ion motion discussed in Sec. 2.2.2, so that the FN mode remains for some time even after the AW has vanished. Eventually, the FN mode vanishes as well for larger wavelengths, and this is due to the fact that the larger assumed wavelength means more collisions within one spatial oscillation of plasma, so neutrals become better coupled to plasma oscillation and have less freedom to move independently following their own forced oscillatory mode. In region C it does not re-appear because of the same reason: we now have propagating AW wave and this is so only because plasma-neutrals mixture is perfectly well coupled, wave period for AW is large enough so particles from the two fluids (ions and neutrals) have time to collide many times in one wave period. They move in concert perfectly well, so that neutrals do not develop their own forced (but independent) motion.

We stress again that the FN oscillation is due to two dimensional dynamics associated with the Alfvén wave which makes the order of the dispersion relation higher. But the FN mode damping is too large (see Fig. 4) so that the mode is not expected to be observed.

All these results are merely for the demonstration, aimed at showing that the multi-component theory in principle may yield results very similar to classic theory, [1] at least regarding the Alfvén wave. So, contrary to recent claims,[7] keeping the Hall term in their hybrid MHD analysis makes no difference; see more on this issue in Appendix A. However, for some parameters the KP solutions may be rather different from the full multi-component theory, and this will be demonstrated in Sec. 3.1.

3 Application to lower solar atmosphere

Full dispersion equation (29) can be applied to solar atmosphere to check the existence of Alfvén waves. As example, for photospheric parameters around the temperature minimum at $h = 490$ km, it is solved in terms of the magnetic field magnitude B_0 for several wavelengths. The densities here are [23] $n_0 = 2.76 \cdot 10^{15} \text{ m}^{-3}$, $n_{n0} = 2.9 \cdot 10^{21} \text{ m}^{-3}$. Using Fig. 1, for the corresponding temperature $T = 4410$ K we have $\sigma_{in,mt} = 376.4 \text{ a.u.}$ which yields $\nu_{in,mt} = 1.84 \cdot 10^7 \text{ Hz}$, and for electrons $\nu_{en} = 2.2 \cdot 10^8 \text{ Hz}$. In order to remain in the proper frequency range, clearly we cannot go to arbitrarily small wave lengths because Ω_i/ω is supposed to be much greater than 1.

The result for the wave lengths $\lambda = 30, 50, 100, 200, 300 \text{ m}$ is presented in Fig. 5. For the given wave lengths the Alfvén wave vanishes for the magnetic field below $B_0 \simeq 0.0804, 0.157, 0.345, 0.705, 1.063 \text{ T}$, respectively. The corresponding wave damping is nearly constant and for the given wave lengths it is $\gamma \simeq 1.3 \cdot 10^7, 1.1 \cdot 10^7, 9.9 \cdot 10^6, 9.45 \cdot 10^6, 9.36 \cdot 10^6 \text{ Hz}$, respectively. Hence, not only that the wave completely vanishes below the given critical magnetic field magnitude, but it is also heavily damped for the magnetic field which formally allows its existence.

Also added in the figure as the top x -axis is the ratio Ω_i/ν_i where $\nu_i \equiv \nu_{i,sc}$ is calculated using the total collision cross section for elastic scattering from Fig. 1 (line 1); for the given temperature ($\simeq 0.38 \text{ eV}$) the cross section is $\sigma_1 = 622.4 \text{ a.u.} = 1.74 \cdot 10^{-18} \text{ m}^{-2}$ so that collision frequency for total scattering is $\nu_{i,sc} = 3.05 \cdot 10^7 \text{ Hz}$. It is seen that the wave vanishes for unmagnetized ions.

In application to strong magnetic structures with the starting magnetic field $B_0(0) = 0.1 \text{ T}$, and assuming that the magnetic field decreases with the altitude as $B_0(x) = \exp[-x/(2h)]$ where $h = 125 \cdot 10^3 \text{ m}$, at the altitude $x = 490 \cdot 10^3 \text{ m}$ its value becomes 0.014 T , and this is well below the required critical values given above. So none of the Alfvén wave wavelengths discussed here can be expected to appear at all, and this holds even if the magnetic field is kept almost constant with the altitude.

Going to shorter wavelengths does not make much sense because the wave frequency becomes close to the gyro-frequency and the theoretical model becomes violated. We have checked this for $\lambda = 15 \text{ m}$ (and for the same other parameters at $h = 490 \text{ km}$ as above), and a strongly damped Alfvén wave is obtained for the magnetic field in the range $0.04 - 0.1 \text{ T}$. For example at $B_0 = 0.04 \text{ T}$ the AW frequency is $\omega_r - i\gamma = 2.5 \cdot 10^6 - i1.6 \cdot 10^7 \text{ Hz}$ while $\Omega_i = 3.8 \cdot 10^6 \text{ Hz}$, so the theory is hardly valid and results are unreliable, though even here the wave vanishes for $B_0 \leq 0.028 \text{ T}$. However, in view of such a great damping, the Alfvén waves in this very short wave length range are unlikely.

The AW propagation for the same wave lengths is checked also at higher altitudes, and the result for $h = 805 \text{ km}$ is given in Fig. 6. The parameters are $T = 5490 \text{ K}$,

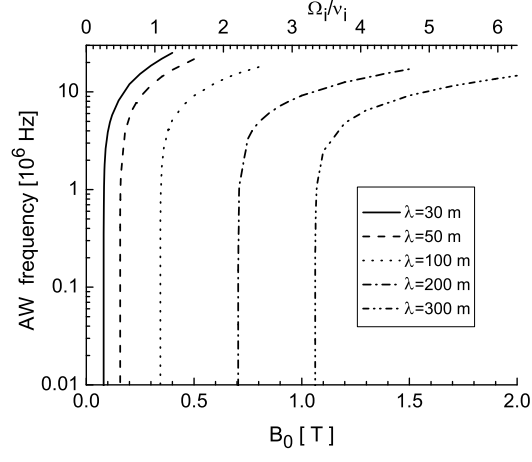


Figure 5: Vanishing of the Alfvén wave frequency, obtained from full dispersion equation (29) for several wavelengths at altitude $h = 490$ km in photosphere, in terms of magnetic field B_0 (bottom axis) and ratio Ω_i/ν_i (top axis).

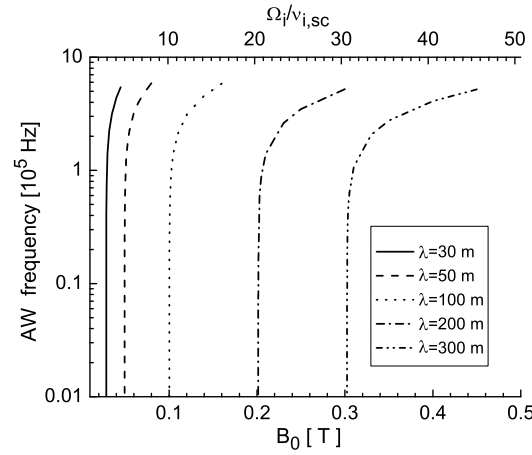


Figure 6: Vanishing of the Alfvén wave frequency, obtained from full dispersion equation (29) for several wave lengths at altitude $h = 805$ km.

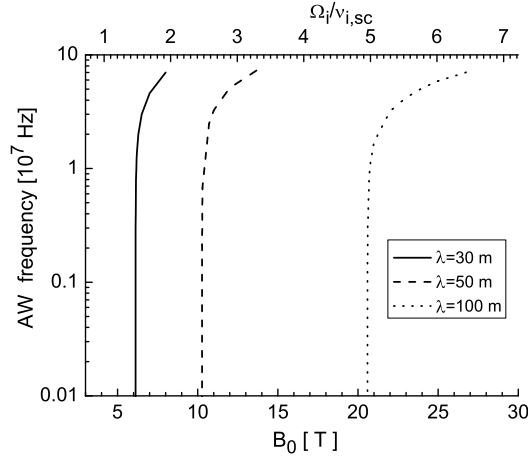


Figure 7: Vanishing of the Alfvén wave frequency, obtained from full dispersion equation (29) at altitude $h = 200$ km.

$n_0 = 8.54 \cdot 10^{16} \text{ m}^{-3}$, $n_{n0} = 1.48 \cdot 10^{20} \text{ m}^{-3}$, and $\nu_{en} = 1.3 \cdot 10^7 \text{ Hz}$. Here, the wave length $\lambda = 30 \text{ m}$ vanishes if the magnetic field is below $B_0 \simeq 0.0285 \text{ T}$, and in this case we still have magnetized protons because $\Omega_i/\nu_i \simeq 3$. Compare this with the wave length $\lambda = 300 \text{ m}$ for which the wave will not appear if the magnetic field is below $B_0 \simeq 0.3 \text{ T}$, for which protons are in fact still strongly magnetized $\Omega_i/\nu_i \simeq 30$. Here again we used the line 1 from Fig 1 which yields $\sigma_1 = 657.24 \text{ a.u.} = 1.84 \cdot 10^{-18} \text{ m}^2$ and the collision frequency for total scattering is $\nu_{i,sc} = 1.83 \cdot 10^6 \text{ Hz}$. The wave damping for all given wave lengths is around $\gamma \simeq 4.7 \cdot 10^5 \text{ Hz}$. Applying this again to the strong flux tubes with the same exponential decrease as above yields the magnetic field at this altitude around 0.004 T only. Therefore none of the wave lengths is expected to appear.

The procedure can be repeated for the layers below the temperature minimum. The number density of neutrals in this area is increased and collision frequencies for protons [11] go over 10^9 Hz . Therefore in order to produce any (strongly damped) Alfvén wave we need tens of T magnetic field. For example, taking the wave length $\lambda = 300 \text{ m}$ it turns out that the required magnetic field at the altitude $h = 200 \text{ km}$ is $B_0 \geq 62 \text{ T}$! The result for wave lengths $\lambda = 30, 50, 100 \text{ m}$ is presented in Fig. 7. The parameters are [23]: $T = 4990 \text{ K}$, $n_0 = 1.1 \cdot 10^{17} \text{ m}^{-3}$, $n_{n0} = 3.47 \cdot 10^{22} \text{ m}^{-3}$, $\nu_{en} = 2.9 \cdot 10^9 \text{ Hz}$, and from Fig. 1 this yields $\nu_{i,sc} = 4 \cdot 10^8 \text{ Hz}$, $\nu_{in,mt} = 1.7 \cdot 10^8 \text{ Hz}$. The AW damping for all three wave lengths is around $8.5 \cdot 10^7 \text{ Hz}$. It is seen that the required magnetic field for the three wave lengths are $B_0 \geq 6.12, 10.27, 20.59 \text{ T}$, respectively, which clearly shows that the Alfvén wave in such an environment is impossible.

Note that the given solutions for AW are accompanied by high frequency waves (32) as well, but being unimportant for the AW behavior those are not presented here. As for the FN oscillations see Sec. 3.1.

In view of these graphs it is very unlikely that the Alfvén wave (which is usually

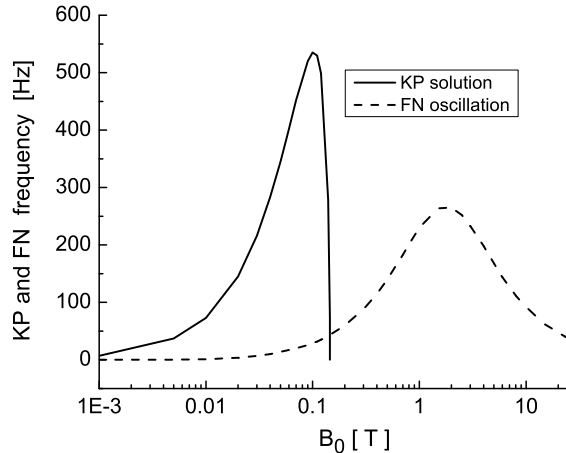


Figure 8: Second propagation window from Kulsrud-Pearce model which allows AW in the photosphere, for $\lambda = 100$ m and for parameters from Fig. 7, and our corresponding FN mode in the same range.

assumed as massively produced by the convective motion in the photosphere and propagating towards the corona) can be used as a tool in explaining the coronal heating. From Figs. 5-7 it is seen that the wave lengths of several tens of meters and longer cannot possibly be excited.

We stress again that the results obtained here follow from the collisional theory summarized in Fig. 1 which provides the most accurate collisional cross sections, where both charge exchange and elastic scattering are consistently taken into account.

3.1 Differences in comparison with the Kulsrud-Pearce solution

Earlier, in Figs. 2, 3 we have demonstrated a perfect agreement (for the Alfvén wave behavior) between our full multi-component model and the Kulsrud-Pearce model. However, this is not generally so, and it turns out to be dependent on parameters. The differences in some cases are in fact profound, and with serious implications. This is shown below.

The Kulsrud-Pearce equation (8) is solved for the same parameters as in Fig. 7 and we compare the cases with $\lambda = 100$ m. In the range of magnetic field from Fig. 7, the KP solution has very similar behavior and vanishes for $B_c < 20.43$ T, so it has a threshold similar to our solutions given above. However, when the magnetic field is further reduced, the KP solution re-appears again at around $B_0 \simeq 0.145$ T, while our AW solution does not exist below the value presented in Fig. 7. Note however that our FN oscillations formally exist below this critical magnetic field value. The FN frequency at B_c is around 40 Hz and its damping around 540 Hz.

This re-appearance of the KP solution is presented in Fig. 8 where we give the real part of KP frequency and of our FN oscillations. The corresponding damping of the KP solution (the graph not presented here) changes from $\gamma_{kp}/\omega_{kp} \simeq 14$ (at $B_0 \simeq 0.145$ T) to

$\gamma_{kp}/\omega_{kp} \simeq 0.007$ at $B_0 = 0.001$ T. So the KP solution behaves completely differently as compared to our AW solution which does not exist in this magnetic field range. The KP line shape in this range is a bit similar to our FN solution. In view of shortcomings of the KP equation discussed in Sec. 2.1, this KP propagation window it is not physical.

The similarity of the KP and our FN mode solutions is much more striking in the following example. We take the altitude $h = 805$ km as in Fig. 6 and solve the KP equation (8) together with our dispersion equation (29) in terms of wave length for a fixed value $B_0 = 0.025$ T. In the short wave length limit, both solutions are practically the same and the wave vanishes at around $\lambda = 25$ m, and this is seen in Fig. 9. Note that in this wavelength range our dispersion equation yields also the FN mode with nearly constant frequency and damping (see the mode presented in Fig. 10 for the whole short and long wavelength range). Our AW solution never re-appears again for longer wave length. However, the KP solution re-appears as shown in Fig. 10. In this long wave length range it clearly coincides with our FN mode, therefore it is not real physical solution for the Alfvén wave. It re-appears only due to earlier explained deficiencies of the MHD model.

On the other hand, the behavior of our FN mode in this wavelength range could be explained as follows. Its damping increases up to some wavelength because of the increased amount of collisions within a FN wave period. The increased real part of FN frequency (up to around 450 m) is because it is driven by two-dimensional ion motion. Yet this ion motion itself, in this range, is sustained only by the imaginary part in AW frequency which increases with wavelength up to some critical value. After this value is achieved, the coupling between two fluids becomes more effective, consequently the AW damping rate decreases and so does the ion two-dimensionality. This in turn affects FN frequency which therefore reduces.

3.1.1 Explanation of differences

The reason why our AW solution does not re-appear in the long wavelength range like in the case of Fig. 3 is clearly related to the magnetization and ionization ratio. In the present case $\Omega_i/\nu_i \simeq 2.5$ while in Fig. 3 this ratio is around 10. So now we have very weakly magnetized ions. The AW vanishes because for these larger wavelength a greater volume of neutrals must be set into motion by colliding ions, which themselves move due to EM perturbations. Hence, having ions so badly magnetized their dragging is not so effective, neutrals thus represent a heavy obstacle and the AW vanishes. For short wavelength there is less amount of collisions with neutrals within one AW wavelength and the AW propagates.

Some more details can be revealed through equations in the following manner. Kulsrud-

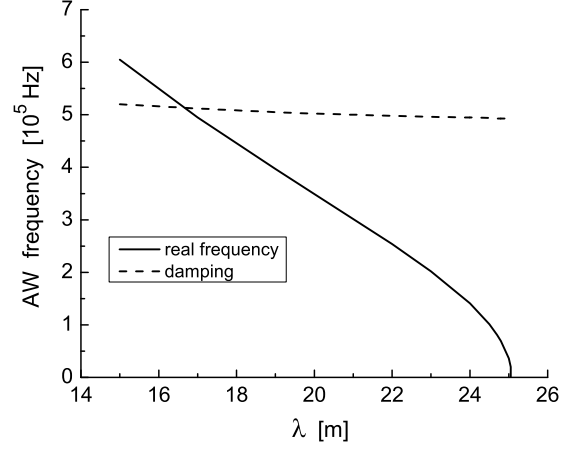


Figure 9: Alfvén wave frequency $\omega = \omega_r - i\gamma$ in short wavelength range from our full multi-component model (29) and Kulsrud-Pearce model (8) at $h = 805$ km and for $B_0 = 0.025$ T.

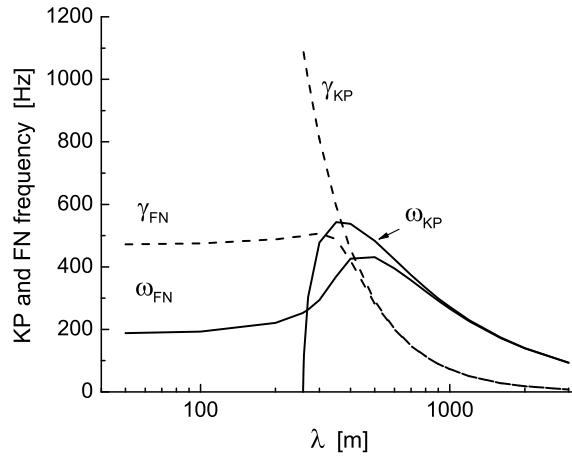


Figure 10: Complete FN mode solution $\omega = \omega_{FN} - i\gamma_{FN}$ corresponding to AW from Fig. 9, and the Kulsrud-Pearce long wavelength range.

Pearce Eq. (8) can be written as:

$$\mathcal{K} \equiv (\omega_1^2 - a^2) (\omega_1 + i\epsilon) + i\omega_1^2 = 0, \quad (34)$$

$$\omega_1 \equiv \frac{\omega}{\nu_{in}}, \quad a^2 = \frac{k^2 c_a^2}{\nu_{in}^2}.$$

We have already shown that our all three equations (22, 24, 29) yield the same solutions, so it is enough to discuss the simplest one, Eq. (22), which can be written as

$$(\omega_1^2 - a^2)(\omega_1 + i\epsilon)^2 + i\omega_1^2(\omega_1 + is) = 0, \quad s = \epsilon + k^2\lambda_i^2. \quad (35)$$

For parameters from Figs. 2, 3 we have $\epsilon = 0.0016$, while $k^2\lambda_i^2 = 0.00007$ in the beginning of the second propagation region C. So $s \simeq \epsilon$, and Eq. (35) for these parameters becomes of the shape:

$$\mathcal{K} \cdot (\omega_1 + i\epsilon) = 0.$$

Hence, our equation clearly has the same or similar AW as solution (with the extra terms which in the end yields the FN mode). This may be seen more clearly for large wavelengths after neglecting a^2 and using the fact that $\epsilon \ll 1$ when Eq. (35) reduces to

$$\omega_1^2 (\omega_1^2 + i\omega_1 - 1) = 0. \quad (36)$$

This equation clearly has two real nontrivial solutions that can only be associated with AW because FN mode is shown numerically to be absent in this wavelength range, and we thus have an agreement with the Kulsrud-Pearce case.

However, for parameters from Figs. 9, 10 we have $\epsilon = 0.00058$, while $k^2\lambda_i^2 = 0.0006$, $k^2\lambda_i^2 = 0.00027$ for wavelengths $\lambda = 200, 300$ m where KP mode re-appears, so $k^2\lambda_i^2$ cannot be omitted and Eq. (35) is written as

$$(\omega_1 + i\epsilon) \cdot \mathcal{K} - \omega_1^2 k^2\lambda_i^2 = 0. \quad (37)$$

We see now that it is the ion inertial length term $k^2\lambda_i^2$ which makes the difference. It naturally appears in multi-component theory while it is absent in KP MHD description [see Eq. (8)]. If it is omitted in our Eqs. (22, 24, 29) we obtain AW behavior similar to KP model, with two propagation windows. Parameters used for Figs. 9, 10 show that it may be greater than the other small term $\epsilon = n_0/n_{n0}$ in Eq. (8) and consequently it cannot always be omitted. Its complete absence in MHD theory has serious consequences: this theory fails to predict the forced neutral mode, and as a result it allows AW in the environment where it cannot exist. We stress that the parameter $k^2\lambda_i^2$ which changes the physics is not introduced on purpose; it just follows from the multicomponent theory in its simplest shape. It is an intrinsic feature of this theory which reflects essential differences between the usual MHD and our derivations.

We can now check the validity of the formula (23) describing the FN mode. For parameters from Figs. 9, 10, and taking wavelength $\lambda = 600$ m, numerical solution of dispersion equation (29) is $\omega_{FN} = 397$ Hz while the formula (23) yields 444 Hz. For $\lambda = 2000$ m the two values are, respectively, 139 Hz and 140 Hz. So the agreement appears to be perfect at long wavelengths. On the other hand, the KP results for the two wavelengths are, respectively, 424 Hz and 139.7 Hz. The formula (23) which describes the neutral mode is obtained after explicitly neglecting terms which yield the Alfvén wave, so its perfect agreement with the KP results is a direct proof that the second propagation window in Kulsrud-Pearce model is not actual physical Alfvén wave. It is in fact associated with the neutral mode as the multi-component theory predicts, yet this cannot be seen from the MHD theory.

4 Conclusions

Full three component analysis given in this work yields results that are partly in agreement with the classical MHD theory citekp and with more recent ones [2, 24] based on the MHD theory. The classic analysis [1] gives two different regimes for propagation of Alfvén waves, first where the wave damping is proportional to the collision frequency, and second which implies an inverse proportionality. Our multi-component analysis in principle confirms such a behavior, contrary to recent claims in [7] that the AW cut-off must vanish if Hall term is included. We have also identified some forced oscillations of the neutral fluid caused by friction with plasma species, which cannot be obtained from the MHD analysis.

However, the agreement of our analysis with [1] depends on particular plasma parameters, and this is demonstrated in Figs. 2, 3 from one side (where the agreement is perfect), and in Figs. 7, 8 (or in Figs. 9, 10) from the other, where some essential differences appear, and those are caused by some intrinsic deficiencies of the MHD model. From these figures it may be concluded that the second propagation window from the Kulsrud-Pearce model (which is correctly described for parameters in Fig. 2), for some other parameters may become un-physical (as it is the case with Fig. 8 and with Fig. 10). The origin of differences is identified: MHD analysis in weakly ionized environment involves one small parameter $\epsilon = n_0/n_{n0}$ while in the same time it misses other small parameter $k^2\lambda_i^2$, which may be of the same order and which is naturally included only through multi-component theory. As an old subject, the Alfvén wave has already been studied experimentally in numerous works in the past, see for example [25], [26], and in particular [27] and [28] dealing with experimental partially ionized plasma; in the present work we have delivered a lot of results that should be kept in mind in eventual future experiments.

From our analysis it follows also that speaking about the Alfvén wave in an environment where ions are un-magnetized is not justified. This is shown partly analytically in

an approximate derivations, and numerically by solving dispersion equation (29) without any approximation. Therefore, the Alfvén wave cannot be excited in an environment like the solar photosphere and this is demonstrated by using specific photospheric parameters and the most accurate collision cross sections that exist. Note that this contradicts the Kulsrud-Pearce model which yields the AW in Fig. 8 in the range where ions are unmagnetized. This shows that the most popular paradigm of the coronal heating by Alfvén waves produced in the photosphere is against physical reality: the ions in the photosphere are unmagnetized [11] and they cannot support the Alfvén wave.

Regarding the work [7] where it is claimed that the AW cut-off is not possible, at this point it is appropriate to make the following comments. They introduce relative perpendicular speed between ions and neutrals $\vec{w}_\perp = \vec{u}_{i\perp} - \vec{u}_{n\perp}$, and the common speed of the two (ions plus neutrals) fluids \vec{u}_\perp . However, they explicitly neglect the time derivative of the relative speed $\partial\vec{w}_\perp/\partial t$, while such a time derivative for the common speed is kept. By neglecting the time variation of the relative speed they have directly *excluded* physical phenomena which develop within transition (collisional) time, and which dictate everything what happens with the mixture of the two fluids (plasma plus neutrals). In other words, the relative motion of neutrals and ions they assume fixed in time. By doing this they prevent the system to evolve freely, and this partly removes effects of friction. Such an assumption is physically unjustified and in view of this it is no surprise that they do not obtain any cut-off. It is also very likely that the FN mode identified in our work is simply overlooked in their work and interpreted as a low frequency continuation of the Alfvén wave (hence the absence of cut-off in their work). Namely, they derive dispersion equation with a free term $\delta_i\nu\xi_i$ (in their own notation), which seems to be equivalent to the free term in our derivation where it yields the FN oscillations.

Acknowledgments: JV is enormously grateful to P. S. Krstic for help and valuable discussions related to the calculation and understanding of collision cross sections which involve quantum-mechanical indistinguishability of colliding particles at low energies.

A On the role of the Hall effect in MHD model

The Hall effect belongs completely to the MHD terminology and it can introduce some new phenomena only within this model, and this when used instead of the ideal Ohm’s law of course. However, the fully multi-component plasma theory used in the present work, being more general, contains all effects that are within the MHD theory normally attributed to the MHD Hall effect, and this will be demonstrated here.

The generalized MHD Ohm’s law, which contains the Hall term, is obtained by combining and re-arranging the momentum equations for plasma components. Our three momentum equations from Sec. 2 can be combined in various ways to obtain the general-

ized Ohm's law. Observe that within the multi-component plasma theory such a combined equation is redundant because we operate with velocities of separate species and not with the current. We may multiply our ion and electron momentum equations by e/m_i and $-e/m_e$, respectively, and then sum the resulting two equations assuming quasi-neutrality, which yields

$$\begin{aligned}
en(\vec{v}_i - \vec{v}_e) = & \sigma \vec{E} + \frac{\sigma}{\beta} \left(\frac{e^2 n}{m_i} \vec{v}_i + \frac{e^2 n}{m_e} \vec{v}_e \right) \times \vec{B} \\
& + \frac{e\sigma}{\beta} \nabla \left(\frac{p_e}{m_e} - \frac{p_i}{m_i} \right) - \frac{\sigma}{\beta} \frac{\partial}{\partial t} [en(\vec{v}_i - \vec{v}_e)] \\
& - \frac{en\sigma}{\beta} [(\vec{v}_i \cdot \nabla) \vec{v}_i - (\vec{v}_e \cdot \nabla) \vec{v}_e] \\
& + \frac{en\sigma}{\beta} [\nu_{en}(\vec{v}_e - \vec{v}_n) - \nu_{in}(\vec{v}_i - \vec{v}_n)].
\end{aligned} \tag{38}$$

Here

$$\sigma = \frac{e^2 n}{m_e \nu_{ei}}, \quad \beta = \frac{e^2 n}{m_i} + \frac{e^2 n}{m_e}.$$

The underlined part of the equation comes from the Lorentz force terms for both electrons and ions, and this part contains the usual MHD Hall term. Indeed, after introducing the total speed of the fluid $(m_i + m_e)\vec{V} = m_i n \vec{v}_i + m_e n \vec{v}_e$, and neglecting only the ion contribution in β (due to mass difference), with simple transformations Eq. (38) becomes

$$\begin{aligned}
\overbrace{en(\vec{v}_i - \vec{v}_e)}^{\vec{j}} = & \sigma \left(\vec{E} + \vec{V} \times \vec{B} \right) + \frac{e}{m_e \nu_{ei}} \nabla \left(p_e - \frac{m_e}{m_i} p_i \right) \\
& - \frac{e}{m_e \nu_{ei}} \overbrace{en(\vec{v}_i - \vec{v}_e)}^{\vec{j}} \times \vec{B} - \frac{1}{\nu_{ei}} \frac{\partial \overbrace{en(\vec{v}_i - \vec{v}_e)}^{\vec{j}}}{\partial t} \\
& - \frac{en}{\nu_{ei}} [(\vec{v}_i \cdot \nabla) \vec{v}_i - (\vec{v}_e \cdot \nabla) \vec{v}_e] \\
& + \frac{en}{\nu_{ei}} [\nu_{en}(\vec{v}_e - \vec{v}_n) - \nu_{in}(\vec{v}_i - \vec{v}_n)].
\end{aligned} \tag{39}$$

Further simplifications are clearly possible but this is not necessary to do because we already see that this equation is the generalized Ohm's law, and the underlined term in Eq. (39) is the well-known MHD Hall term. The origin of the Hall term and the $\vec{V} \times \vec{B}$ term is in the Lorentz force. This equation contains the velocities of ions and electrons, and it must be complemented with any of the two used momentum equations in order to have a closed set of equations. Such a new set will again contain exactly the same physics, and it will again yield the same dispersion equation given in the Appendix B.

This manipulation with momentum equations can be done differently, by adding all three momentum equations (for electrons, ions and neutrals). But as above, this equation must then be complemented by two of the starting three equations to close the set, and the

resulting dispersion equation will again be the same as if this manipulation of momentum equations is not used at all.

It may be concluded that our multi-component equations contain all physics equivalent to the Hall effect within the MHD theory. Nevertheless, with all this we are still able to recover the classic KP results as shown in Fig. 3 in Sec. 2.4.1. This additionally shows that recent claims [7] of new phenomena introduced by the Hall effect, which apparently remove the classic KP cut-off, cannot possibly be correct, and the Hall effect does not change the classic Kulsrud-Pearce result. Reality is that the essential new phenomena which make the difference arise from the fact that the more complete dispersion equation derived in our work contains additional small parameter with the ion inertial length, and this is unrelated to the Hall term.

B Dispersion equation for collisional Alfvén wave in three-component plasmas

Dispersion equation (29) in explicit form reads:

$$a_6\omega^6 + ia_5\omega^5 - a_4\omega^4 - ia_3\omega^3 + a_2\omega^2 + ia_1\omega - a_0 = 0. \quad (40)$$

After neglecting only terms with m_e/m_i with respect to 1 (some additional simplifications are clearly possible), the coefficients read:

$$\begin{aligned} a_0 &= \Omega_i^2 \Omega_e^2 k^2 \lambda_e^2 \frac{n_0^2}{n_{n0}^2} \left(\nu_{in} + \nu_{en} \frac{m_e}{m_i} \right)^2, \quad \lambda_e = \frac{c}{\omega_{pe}}, \\ a_1 &= 2k^2 \lambda_e^2 \Omega_i^2 \frac{m_e^2}{m_i^2} \frac{n_0^2}{n_{n0}^2} \left(\nu_{en} + \nu_{in} \frac{m_i}{m_e} \right) \{ \nu_{ei} \nu_{en} \\ &\quad + \Omega_e^2 \frac{m_i}{m_e} \frac{n_{n0}}{n_0} + \frac{m_i^2}{m_e^2} \left(1 + \frac{n_{n0}}{n_0} \right) \nu_{in} (\nu_{ei} + \nu_{en}) \\ &\quad + \frac{m_i}{m_e} [\nu_{en} \nu_{in} + \nu_{ei} (\nu_{en} + \nu_{in}) + \nu_{ei} \nu_{en} \frac{n_{n0}}{n_0}] \}, \\ a_2 &= \Omega_i^2 \frac{n_0^2}{n_{n0}^2} \left[\left(\nu_{en}^2 \frac{m_e}{m_i} + 2\nu_{en} \nu_{in} \right) \left(1 + \frac{n_{n0}}{n_0} \right) \right. \\ &\quad \left. + \nu_{in}^2 \left(1 + \frac{m_i}{m_e} \left(1 + \frac{n_{n0}}{n_0} \right) \right) \right] + \Omega_i^2 k^2 \lambda_e^2 \{ \Omega_e^2 \\ &\quad + 2\nu_{ei} \nu_{en} \left(1 + \frac{2n_{n0}}{n_0} \right) + \nu_{en}^2 \left[\left(1 + \frac{m_e}{m_i} \frac{n_0}{n_{n0}} \right)^2 + \frac{n_0^2}{n_{n0}^2} \right] \right. \\ &\quad \left. + \nu_{in}^2 \left[\frac{m_i^2}{m_e^2} \left(1 + \frac{n_0}{n_{n0}} \right)^2 + \frac{n_0^2}{n_{n0}^2} \right] \right. \\ &\quad \left. + 2\nu_{en} \nu_{in} \frac{n_0^2}{n_{n0}^2} \left[\frac{m_i}{m_e} \left(1 + \frac{2n_{n0}}{n_0} \right) + \frac{2n_{n0}}{n_0} \right] + 4\nu_{ei} \nu_{in} \frac{m_i}{m_e} \frac{n_0}{n_{n0}} \right\} \end{aligned}$$

$$\begin{aligned}
& +k^2\lambda_e^2 \left\{ \nu_{in}^2 (\nu_{en}^2 + \nu_{ei}^2) \left(1 + \frac{n_0}{n_{n0}}\right)^2 \right. \\
& + \nu_{ei}^2 \nu_{en}^2 \frac{m_e^2}{m_i^2} \left[\left(1 + \frac{2m_e}{m_i} \frac{n_0^2}{n_{n0}^2} + \frac{n_0^2}{n_{n0}^2}\right) + 2\frac{n_0}{n_{n0}} \right] \\
& + 2\nu_{ei}\nu_{in}\nu_{en}^2 \frac{m_e}{m_i} \frac{n_0}{n_{n0}} \left(2 + \frac{n_0}{n_{n0}}\right) \\
& + \frac{2m_e}{m_i} (\nu_{en}\nu_{in}\nu_{ei}^2 + \nu_{ei}\nu_{in}\nu_{en}^2) + 2\nu_{ei}\nu_{en}\nu_{in}^2 \left(1 + \frac{n_0^2}{n_{n0}^2}\right) \\
& \left. + 2\nu_{en}\nu_{in}\nu_{ei}^2 \frac{m_e}{m_i} \frac{n_0}{n_{n0}} \left(4 + \frac{n_0}{n_{n0}}\right) + \frac{4n_0}{n_{n0}} \nu_{ei}\nu_{en}\nu_{in}^2 \right\}, \\
a_3 = & \Omega_i^2 \left\{ \left(\nu_{en} + \nu_{in} \frac{m_i}{m_e} \right) \left(1 + \frac{2n_0}{n_{n0}}\right) + 2k^2\lambda_e^2 \left[\nu_{ei} \frac{m_i}{m_e} \right. \right. \\
& + \nu_{en} \left(1 + \frac{m_i}{m_e} \frac{n_0}{n_{n0}}\right) + \nu_{in} \left(\frac{n_0}{n_{n0}} + \frac{m_i^2}{m_e^2} \left(1 + \frac{n_0}{n_{n0}}\right) \right) \left. \right] \left. \right\} \\
& + (\nu_{ei} + \nu_{en})\nu_{in}^2 + \nu_{en}^2 \frac{m_e}{m_i} \left[\nu_{in} + \nu_{ei} \frac{m_e}{m_i} \left(1 + \frac{n_0^2}{n_{n0}^2}\right) \right] \\
& + 2\nu_{ei}\nu_{en}^2 \frac{n_0}{n_{n0}} \frac{m_e^2}{m_i^2} \left(1 + \frac{n_0}{n_{n0}} \frac{m_e}{m_i}\right) + \nu_{in}\nu_{en}^2 \frac{m_e}{m_i} \left(1 + \frac{2n_0}{n_{n0}}\right) \\
& + 2\nu_{ei}\nu_{en}\nu_{in} \frac{m_e}{m_i} \left(1 + \frac{n_0}{n_{n0}}\right)^2 + (\nu_{ei} + \nu_{en})\nu_{in}^2 \frac{n_0}{n_{n0}} \left(2 + \frac{n_0}{n_{n0}}\right) \\
& + 2k^2\lambda_e^2 \left\{ \frac{m_e}{m_i} (\nu_{ei} + \nu_{en})\nu_{ei}\nu_{en} + \nu_{in}\nu_{ei}^2 + \nu_{in}\nu_{en}^2 + \nu_{ei}\nu_{in}^2 \right. \\
& + \nu_{en}\nu_{in}^2 + 2\nu_{ei}\nu_{en}\nu_{in} + \frac{n_0^2}{n_{n0}^2} \left[\nu_{en}\nu_{in}^2 + \nu_{ei}\nu_{in}^2 + \nu_{in}\nu_{en} \frac{m_e}{m_i} \right. \\
& + \nu_{ei}\nu_{en}^2 \frac{m_e^2}{m_i^2} + 2\nu_{ei}\nu_{en}\nu_{in} \frac{m_e}{m_i} \left. \right] + \frac{2n_0}{n_{n0}} \left[\nu_{ei}\nu_{en}\nu_{in} + \nu_{in}^2 (\nu_{ei} + \nu_{en}) \right] \\
& \left. + \nu_{in} (\nu_{ei}^2 + \nu_{en}^2) \frac{n_0}{n_{n0}} + \nu_{ei}\nu_{en} (\nu_{ei} + \nu_{en}) \frac{m_e}{m_i} \frac{n_0}{n_{n0}} \right\}, \\
a_4 = & \Omega_e\Omega_i + \Omega_e^2 k^2 \lambda_e^2 + \nu_{in}^2 \left(1 + \frac{n_0}{n_{n0}}\right)^2 + 2\nu_{ei}\nu_{en} \frac{m_e}{m_i} \left(1 + \frac{n_0}{n_{n0}}\right) \\
& + \nu_{en}^2 \frac{m_e}{m_i} \left[1 + \frac{n_0}{n_{n0}} \left(1 + \frac{m_e}{m_i} \frac{n_0}{n_{n0}}\right) \right] + 2\nu_{ei}\nu_{in} \left(1 + \frac{n_0}{n_{n0}}\right) \\
& + 2\nu_{en}\nu_{in} \left[1 + \frac{n_0}{n_{n0}} \left(1 + \frac{m_e}{m_i} \frac{n_0}{n_{n0}}\right) \right] \\
& + k^2\lambda_e^2 \left\{ \nu_{ei}^2 + \nu_{in}^2 \left(1 + \frac{n_0}{n_{n0}}\right)^2 + \nu_{en}^2 \left[1 + \frac{m_e}{m_i} \frac{n_0}{n_{n0}} \right. \right. \\
& + \frac{m_e}{m_i} \frac{n_0}{n_{n0}} \left. \right] + 2\nu_{ei}\nu_{en} \left(1 + \frac{2m_e}{m_i} \frac{n_0}{n_{n0}}\right) + 4\nu_{ei}\nu_{in} \left(1 + \frac{n_0}{n_{n0}}\right) \\
& \left. + 2\nu_{en}\nu_{in} \left[2 + \frac{n_0}{n_{n0}} \left(2 + \frac{m_e}{m_i} \frac{n_0}{n_{n0}}\right) \right] \right\},
\end{aligned}$$

$$\begin{aligned}
a_5 &= \nu_{ei} \left(1 + 2k^2 \lambda_e^2\right) + 2\nu_{in} \left[1 + \frac{n_0}{n_{n0}} + k^2 \lambda_e^2 \left(1 + \frac{n_0}{n_{n0}}\right)\right] \\
&\quad + \nu_{en} \left[1 + \frac{2m_e}{m_i} \frac{n_0}{n_{n0}} + 2k^2 \lambda_e^2 \left(1 + \frac{m_e}{m_i} \frac{n_0}{n_{n0}}\right)\right], \\
a_6 &= 1 + k^2 \lambda_e^2.
\end{aligned}$$

We stress that in the present work we have used full dispersion equation (29) without approximations (with complete electron contribution), instead of Eq. (40) with the approximate coefficients a_j given above.

References

- [1] R. Kulsrud and W. P. Pearce, *Astrophys. J.* **156**, 445 (1969).
- [2] R. E. Pudritz, *Astrophys. J.* **350**, 195 (1990).
- [3] N. Kumar and B. Roberts, *Solar Phys.* **214**, 241 (2003).
- [4] R. Soler, M. Carbonell, J. L. Ballester, and J. Terradas, *Astrophys. J.* **767**, 171 (2013).
- [5] Y. T. Tsap, A. V. Stepanov, and Y. T. Kopylova, *Solar Phys.* **270**, 205 (2011).
- [6] J. Vranjes, S. Poedts, B. P. Pandey, and B. De Pontieu, *Astron. Astrophys.* **478**, 553 (2008).
- [7] T. V. Zaqarashvili, M. Carbonell, J. L. Ballester, and M. L. Khodachenko, *Astron. Astrophys.* **544**, A143 (2012).
- [8] P. S. Krstic and D. R. Schultz, *Atomic and Plasma-Material Interaction Data for Fusion, Vol. 8* (IAEA, Vienna, 1998).
- [9] P. S. Krstic and D. R. Schultz, *J. Phys. B: At. Mol. Opt. Phys.* **32**, 3485 (1999).
- [10] P. S. Krstic and D. R. Schultz, *Phys. Rev. A* **60**, 2118 (1999).
- [11] J. Vranjes and P. S. Krstic, *Astron. Astrophys.* **554**, A22 (2013).
- [12] A. E. Glassgold, P. S. Krstic and D. R. Schultz, *Astrophys. J.* **621**, 808 (2005).
- [13] D. R. Schultz, P. S. Krstic, T. G. Lee, and J. C. Raymond, *Astrophys. J.* **678**, 950 (2008).
- [14] Y. P. Raizer, *Gas Discharge Physics* (Springer-Verlag, Berlin Heidelberg, 1991).
- [15] N. Vargaftik, Y. K. Vinogradov, and V. S. Yargin, *Handbook of Physical Properties of Liquids and Gases* (Begell House, New York, 1996).

- [16] A. Dalgarno, M. Yan, and W. Liu, *Astrophys. J. Suppl.* **125**, 237 (1999).
- [17] F. F. Chen, *Introduction to Plasma Physics and Controlled Fusion* (Plenum Press, New York, 1988).
- [18] P. J. Catto, *Phys. Plasmas* **1**, 1936 (1994).
- [19] P. Helander, S. I. Krasheninnikov, and P. J. Catto, *Phys. Plasmas* **1**, 3174 (1994).
- [20] P. M. Bellan, *Phys. Plasmas* **1**, 3523 (1994).
- [21] J. Vranjes and S. Poedts, *Phys. Plasmas* **17**, 022104 (2010).
- [22] W. G. Roberge and G. E. Ciolek, *MNRAS* **382**, 717 (2007).
- [23] J. M. Fontenla, E. H. Avrett, and R. Loeser, *Astrophys. J.* **406**, 319 (1993).
- [24] O. M. Blaes and S. A. Balbus, *Astrophys. J.* **421**, 163 (1994).
- [25] A. Gigliotti, W. Gekelman, P. Pribyl, S. Vincena, A. Karavaev, X. Shao, A. Surjalal Sharma, and D. Papadopoulos, *Phys. Plasmas* **16**, 092106 (2009).
- [26] S. T. Vincena, G. J. Morales, and J. E. Maggs, *Phys. Plasmas* **17**, 052106 (2010).
- [27] C. Watts and J. Hanna, *Phys. Plasmas* **11**, 1358 (2004).
- [28] W. Gekelman, S. Vincena, B. Van Compernelle, G. J. Morales, J. E. Maggs, P. Pribyl, and T. A. Carter, *Phys. Plasmas* **18**, 055501 (2011).